NATIONAL ADVISORY COMMITTEE FOR AERONAUTICS

REPORT No. 478

EXPERIMENTAL VERIFICATION OF THE THEORY OF WIND-TUNNEL BOUNDARY INTERFERENCE

By THEODORE THEODORSEN and ABE SILVERSTEIN

1934

AERONAUTIC SYMBOLS

1. FUNDAMENTAL AND DERIVED UNITS

	Symbol	Metric		English	
		Unit	Abbreviation	Unit	Abbreviation
Length	l	meter	m	foot (or mile)	ft. (or mi.)
Time	t	second	s	second (or hour)	sec. (or hr.)
Force	F	weight of 1 kilogram	kg	weight of 1 pound	lb.
Power	P	horsepower (metric)		horsepower	hp.
Speed	V	kilometers per hour	k.p.h.	miles per hour	m.p.h.
		meters per second	m.p.s.	feet per second	f.p.s.

2. GENERAL SYMBOLS

W, Weight $= mg$

g, Standard acceleration of gravity $= 9.80665$ m/s² or 32.1740 ft./sec.²

m, Mass $= \dfrac{W}{g}$

I, Moment of inertia $= mk^2$. (Indicate axis of radius of gyration k by proper subscript.)

μ, Coefficient of viscosity

ν, Kinematic viscosity

ρ, Density (mass per unit volume)

Standard density of dry air, 0.12497 kg-m⁻⁴-s² at 15° C. and 760 mm; or 0.002378 lb.-ft.⁻⁴ sec.²

Specific weight of "standard" air, 1.2255 kg/m³ or 0.07651 lb./cu.ft.

3. AERODYNAMIC SYMBOLS

S, Area

S_w, Area of wing

G, Gap

b, Span

c, Chord

$\dfrac{b^2}{S}$, Aspect ratio

V, True air speed

q, Dynamic pressure $= \dfrac{1}{2}\rho V^2$

L, Lift, absolute coefficient $C_L = \dfrac{L}{qS}$

D, Drag, absolute coefficient $C_D = \dfrac{D}{qS}$

D_o, Profile drag, absolute coefficient $C_{D_o} = \dfrac{D_o}{qS}$

D_i, Induced drag, absolute coefficient $C_{D_i} = \dfrac{D_i}{qS}$

D_p, Parasite drag, absolute coefficient $C_{D_p} = \dfrac{D_p}{qS}$

C, Cross-wind force, absolute coefficient $C_C = \dfrac{C}{qS}$

R, Resultant force

i_w, Angle of setting of wings (relative to thrust line)

i_t, Angle of stabilizer setting (relative to thrust line)

Q, Resultant moment

Ω, Resultant angular velocity

$\rho\dfrac{Vl}{\mu}$, Reynolds Number, where l is a linear dimension (e.g., for a model airfoil 3 in. chord, 100 m.p.h. normal pressure at 15° C., the corresponding number is 234,000; or for a model of 10 cm chord, 40 m.p.s. the corresponding number is 274,000)

C_p, Center-of-pressure coefficient (ratio of distance of c.p. from leading edge to chord length)

α, Angle of attack

ϵ, Angle of downwash

α_o, Angle of attack, infinite aspect ratio

α_i, Angle of attack, induced

α_a, Angle of attack, absolute (measured from zero-lift position)

γ, Flight-path angle

REPORT No. 478

EXPERIMENTAL VERIFICATION OF THE THEORY OF WIND-TUNNEL BOUNDARY INTERFERENCE

By THEODORE THEODORSEN and ABE SILVERSTEIN

Langley Memorial Aeronautical Laboratory

NATIONAL ADVISORY COMMITTEE FOR AERONAUTICS

HEADQUARTERS, NAVY BUILDING, WASHINGTON, D.C.

LABORATORIES, LANGLEY FIELD, VA.

Created by act of Congress approved March 3, 1915, for the supervision and direction of the scientific study of the problems of flight. Its membership was increased to 15 by act approved March 2, 1929. The members are appointed by the President, and serve as such without compensation.

JOSEPH S. AMES, Ph.D., *Chairman*,
    President, Johns Hopkins University, Baltimore, Md.
DAVID W. TAYLOR, D.Eng., *Vice Chairman*,
    Washington, D.C.
CHARLES G. ABBOT, Sc.D.,
    Secretary, Smithsonian Institution.
LYMAN J. BRIGGS, Ph.D.,
    Director, Bureau of Standards.
ARTHUR B. COOK, Captain, United States Navy,
    Assistant Chief, Bureau of Aeronautics, Navy Department.
BENJAMIN D. FOULOIS, Major General, United States Army,
    Chief of Air Corps, War Department.
HARRY F. GUGGENHEIM, M.A.,
    Port Washington, Long Island, N.Y.
ERNEST J. KING, Rear Admiral, United States Navy,
    Chief, Bureau of Aeronautics, Navy Department.

CHARLES A. LINDBERGH, LL.D.,
    New York City.
WILLIAM P. MACCRACKEN, Jr., Ph.B.,
    Washington, D.C.
CHARLES F. MARVIN, Sc.D.,
    United States Weather Bureau.
HENRY C. PRATT, Brigadier General, United States Army,
    Chief, Matériel Division, Air Corps, Wright Field, Dayton, Ohio.
EUGENE L. VIDAL, C.E.,
    Director of Aeronautics, Department of Commerce.
EDWARD P. WARNER, M.S.,
    Editor of Aviation, New York City.
ORVILLE WRIGHT, Sc.D.,
    Dayton, Ohio.

GEORGE W. LEWIS, *Director of Aeronautical Research*

JOHN F. VICTORY, *Secretary*

HENRY J. E. REID, *Engineer in Charge, Langley Memorial Aeronautical Laboratory, Langley Field, Va.*

JOHN J. IDE, *Technical Assistant in Europe, Paris, France*

TECHNICAL COMMITTEES

AERODYNAMICS
POWER PLANTS FOR AIRCRAFT
MATERIALS FOR AIRCRAFT

PROBLEMS OF AIR NAVIGATION
AIRCRAFT ACCIDENTS
INVENTIONS AND DESIGNS

Coordination of Research Needs of Military and Civil Aviation

Preparation of Research Programs

Allocation of Problems

Prevention of Duplication

Consideration of Inventions

LANGLEY MEMORIAL AERONAUTICAL LABORATORY

LANGLEY FIELD, VA.

Unified conduct for all agencies of scientific research on the fundamental problems of flight.

OFFICE OF AERONAUTICAL INTELLIGENCE

WASHINGTON, D.C.

Collection, classification, compilation, and dissemination of scientific and technical information on aeronautics.

REPORT No. 478

EXPERIMENTAL VERIFICATION OF THE THEORY OF WIND-TUNNEL BOUNDARY INTERFERENCE

By Theodore Theodorsen and Abe Silverstein

SUMMARY

The results of an experimental investigation on the boundary-correction factor, conducted at the N.A.C.A. laboratories at Langley Field, Va., are presented in this report. The values of the boundary-correction factor from the theory, which at the present time is virtually completed, are given in the paper for all conventional types of tunnels.

With the isolation of certain disturbing effects, the experimental boundary-correction factor was found to be in satisfactory agreement with the theoretically predicted values, thus verifying the soundness and sufficiency of the theoretical analysis. The establishment of a considerable velocity distortion, in the nature of a unique blocking effect, constitutes a principal result of the investigation.

The major portion of the investigation was carried on in the N.A.C.A. full-scale wind tunnel, which afforded the unusual opportunity of a direct comparison with flight results as a final verification.

INTRODUCTION

A number of theoretical papers have recently appeared on the subject of wind-tunnel interference. The theory has in particular been extended to include the effect of a finite airfoil span. The correction factors are available for all ordinary types of tunnels and all airfoil spans. The curves presented in figure 1 embrace virtually all important results on the boundary-correction factors. The curves for the open and closed elliptical sections are taken from a recent paper by Tani and Sanuki (reference 1); the curve for the correction factor of the closed rectangular tunnel from a paper by Glauert (reference 2), the results of which have been extended to cover intermediate cases; while the final case of the open rectangular tunnel is taken from a paper by one of the authors (reference 3).

It remained to be shown whether experimental agreement with the theory existed. A paper by Knight and Harris on open-throat wind tunnels (reference 4), which was the only extensive experimental material available on the subject, gave an indication of conflicting results, inasmuch as the drag correction seemed to differ from the lift correction and no consistent agreement with the theory was obtained.

About 2 years ago a paper by one of the authors (reference 5) appeared on the correction factor for several special types of rectangular tunnels. Cases of zero wall interference were predicted [1] (fig. 2), and it was at the time decided to subject not only these, but the entire problem of boundary interference, to an extensive experimental study to verify the theory. This information became even more desirable with the construction of the full-scale tunnel.

This tunnel (reference 6) afforded the unique opportunity of measuring characteristics of airplanes at large Reynolds Numbers. The fact that accurate flight results were available for these airplanes permitted a critical checking of the corrected wind-tunnel characteristics. Any test errors or disregarded influences immediately revealed themselves, which served materially to guide the course and nature of the following investigations, and led to important conclusions.

The experiments on the boundary-interference factor were started originally in a 2- by 4-foot experimental model of the N.A.C.A. full-scale tunnel. The model tunnel was rebuilt with various modifications of the test section. Some tests were also conducted with the airfoils at various heights in the original open-throat model tunnel. This case has also been treated theoretically in reference 1, and typical numerical examples have been worked out in figure 3, which refers to airfoils of 40, 50, 60, and 70 percent spans at various heights in the full-scale tunnel and its model.

The experimental results from the model tunnel showed conflicting tendencies similar to those observed in reference 4. It is obvious that in tests of this nature the greatest accuracy is required; however, the inconsistencies persisted in spite of numerous refinements and checkings. The investigation was next extended to the full-scale tunnel. The preliminary results in the full-scale tunnel again conflicted with the theory;

---

[1] Glauert called attention to certain errors in these results; for the corrected values, see Rosenhead: Interference Due to a Wind Tunnel, Proceedings of the Royal Society, Oct. 2, 1933.
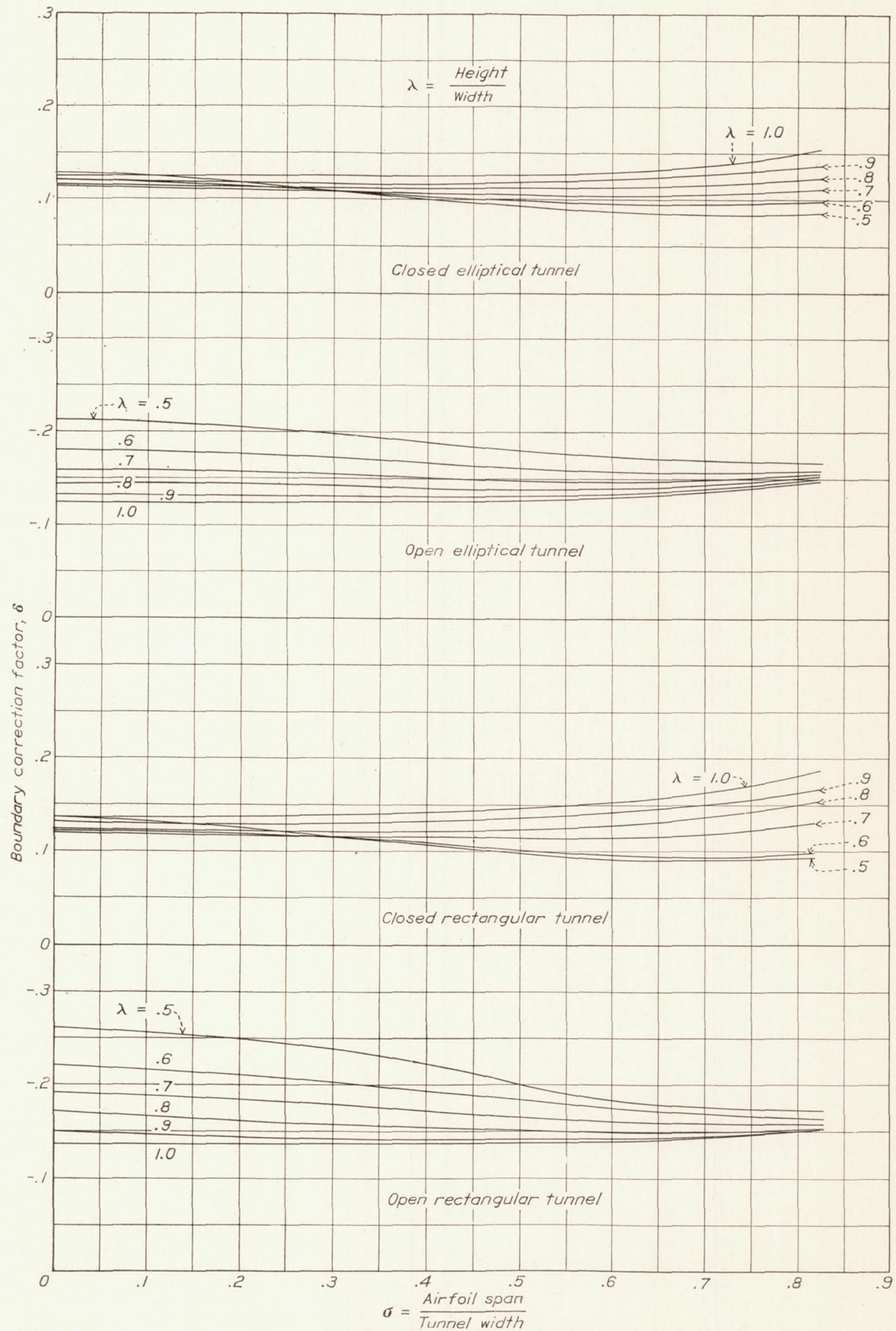
FIGURE 1.—Theoretical boundary correction factors for airfoils of finite span in conventional tunnel sections.

moreover, the corrected characteristics did not agree with flight results, indicating the presence of certain disturbing influences. The nature of these was finally
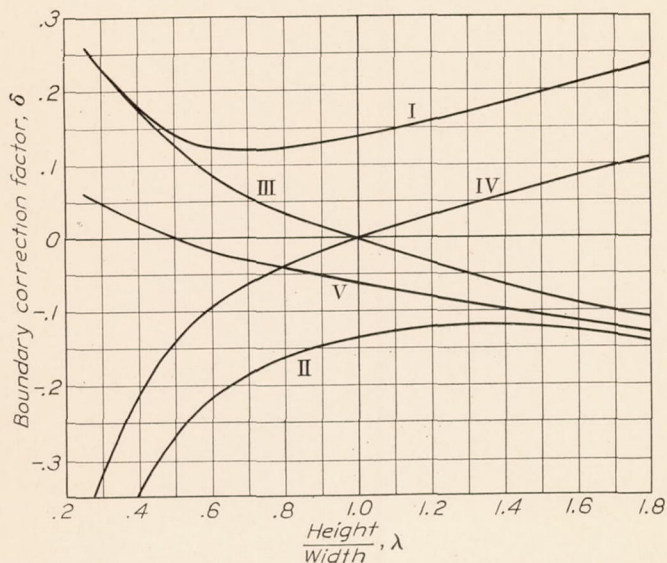

FIGURE 2.—Theoretical boundary correction factors for five types of rectangular tunnels (infinitely small airfoils). I, closed tunnel; II, free jet; III, horizontal boundaries; IV, vertical boundaries; V, one horizontal boundary.
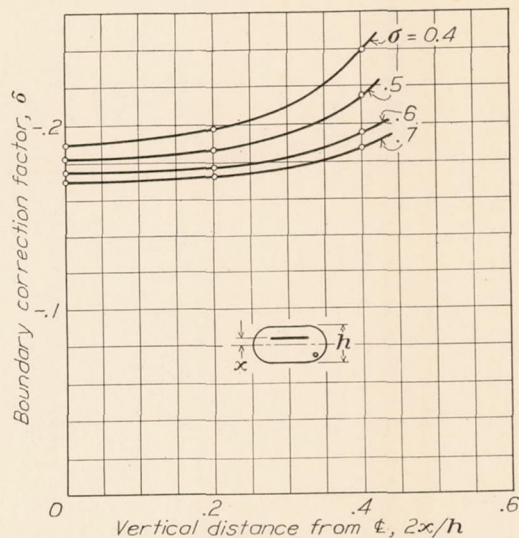
disclosed and their effects are included in the results. The material is presented in chronological order.

The authors wish to extend their acknowledgment to Mr. Smith J. DeFrance, under whose supervision the

model tunnel is not an exact scale model of the final full-scale tunnel, owing to changes incorporated into the design of the large tunnel as a result of experience

FIGURE 3.—Theoretical boundary correction factor for off-center positions of airfoils with $\sigma = 0.4$, 0.5, 0.6, and 0.7 in an open elliptical tunnel (2:1 ellipse).

with the model. The entrance and exit cones of the model are, however, geometrically similar to those of the full-scale tunnel.

The model is an open-throat double-return-passage tunnel (fig. 4) with a jet cross section of 2 by 4 feet
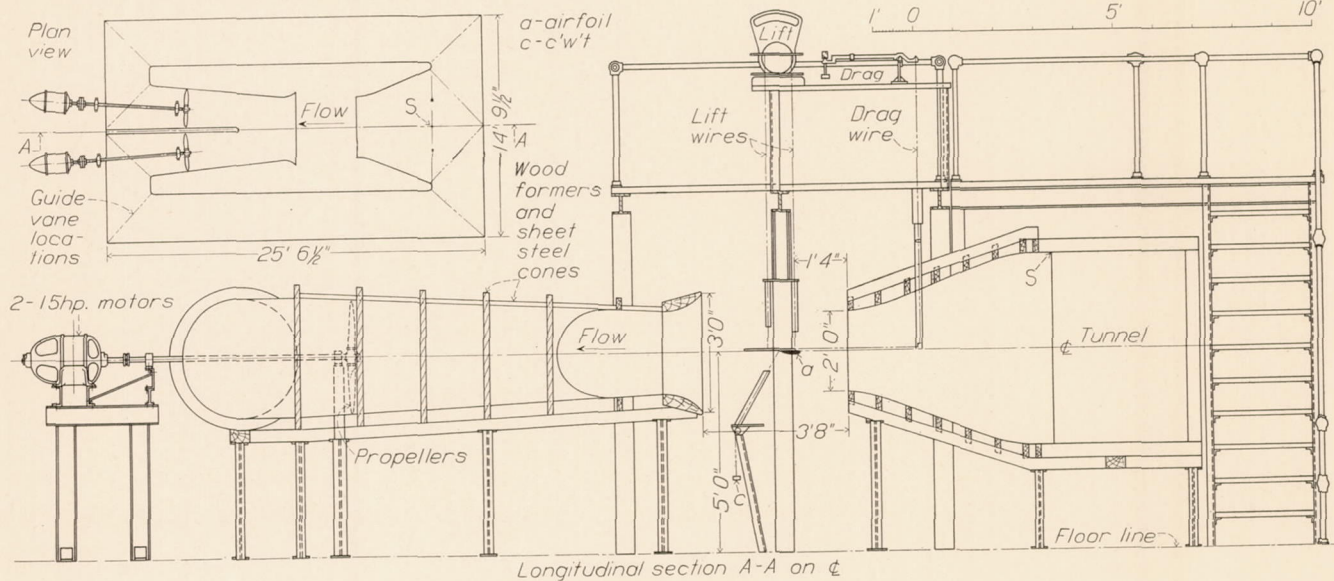
FIGURE 4.—Plan and elevation of model tunnel.

tests in the full-scale tunnel were conducted and whose generous cooperation greatly facilitated the work.

MODEL TUNNEL INVESTIGATION

Tunnel and equipment.—The 1/15-scale model of the full-scale wind tunnel, in which the first test series was conducted, was built at the time the large tunnel was being designed to provide general knowledge of the air-flow characteristics and design information. The

with parallel top and bottom and semicircular ends (fig. 5). The air is circulated by two propellers, each absorbing 15 horsepower at full load, driven by 2 direct-current motors. An area reduction of approximately 5 : 1 is effected in the double curved entrance cone. A collector bell is attached to the mouth of the exit cone, and the tunnel cross section increases almost uniformly from this point to the mouth of the entrance cone. A maximum velocity of about 85 miles per hour

is attainable, and rheostats on the motors permit control to a minimum speed of 5 miles per hour. The energy ratio at maximum speed is 1.5. The dynamic

FIGURE 5.—Experimental set-up of Clark Y airfoil in model tunnel.

pressure at any point within the working portion of the jet is within 1 percent of the average value, and the direction of flow is within ± ½° of the tunnel axis.
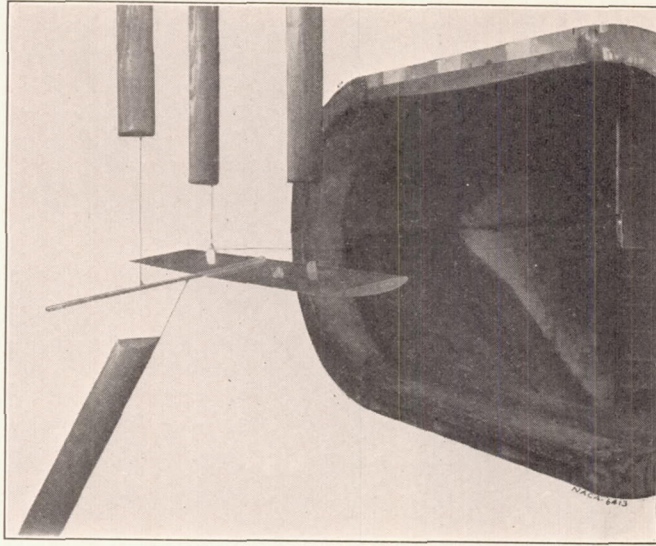
ing between a static pressure orifice in the entrance cone and the room pressure, which differential is measured on a standard N.A.C.A. micromanometer. The dynamic pressure is obtained by calibration of this differential pressure against a standard pitot tube; with the fairings for particular set-ups in position, pitot surveys are made across the area to be occupied by the airfoil and from an average of these surveys the calibration factor computed. The location of the static orifice is shown by S in figure 4.

A wire balance (figs. 5 and 6) is used to measure the forces on the airfoils. The vertical forces are transmitted to the lift scale overhead by three wires, the front two of which are connected by streamline lugs to the airfoil proper and the rear one is connected to a sting. A V-wire yoke connected to the same lugs and extending forward into the entrance cone is used to transmit the drag force. A single wire is connected between the apex of the V and the bell crank in the drag strut, from which point the drag force is transmitted upward to the scale. A counterweight, used to hold the proper tension in the wires, is connected through a wire to the airfoil sting. A pendulum-type dial scale is used to measure the lift, and a beam scale is used for the drag. The angle of attack is measured
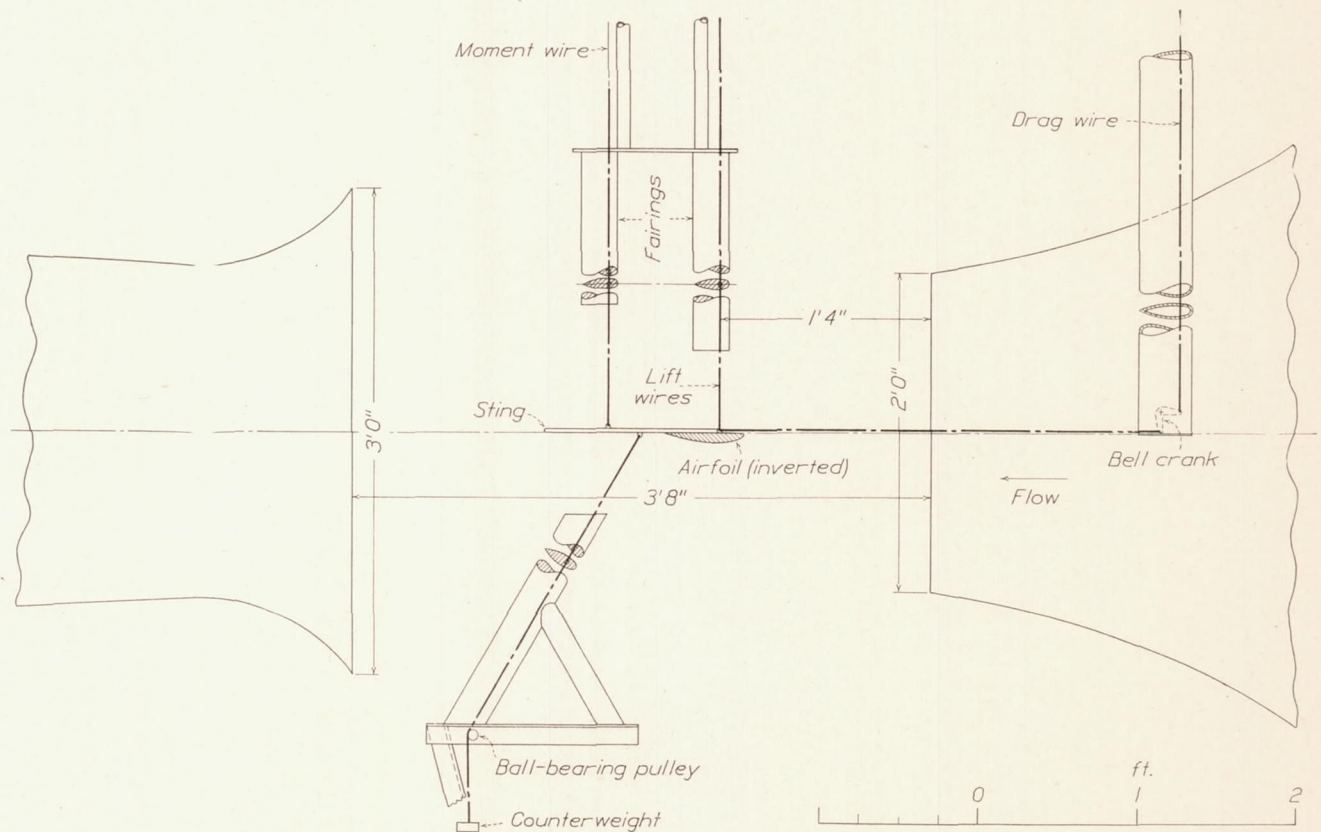
FIGURE 6.—Arrangement of airfoil on balance in model tunnel.

The static pressure gradient along the axis of the jet is approximately zero in the region in which the airfoils were tested. The dynamic pressure at the test body is indicated by means of the differential pressure existing by a sensitive inclinometer, the precision being in the order of ± 0.05°. The tare drag is reduced to a minimum by the use of fairings over the wires. These fairings are dimensioned in sizes proportional to the

airfoil chords and, through the additional precaution of scaling all wires and fittings in these same proportions, practically the same tare drag coefficient is present with all set-ups.

Four duralumin Clark Y airfoils were used as standards throughout the entire test series in the model tunnel. These airfoils were of 3-, 4-, 5-, and 6-inch chords, and of aspect ratio 6. Since small inaccuracies in the airfoil sections in certain critical locations are detrimental to the precision of the tests,

S is the airfoil area and C is the cross-sectional area of the jet. In accordance with this definition, the values of $\Delta\alpha$, ΔC_D, and the correction factor δ are positive for the closed tunnel and negative for the open.

The routine procedure for obtaining the experimental boundary correction δ involves the plotting of characteristics with the extrapolation to free-air conditions. These plots for the model-tunnel tests have not been included and, in order to illustrate the method
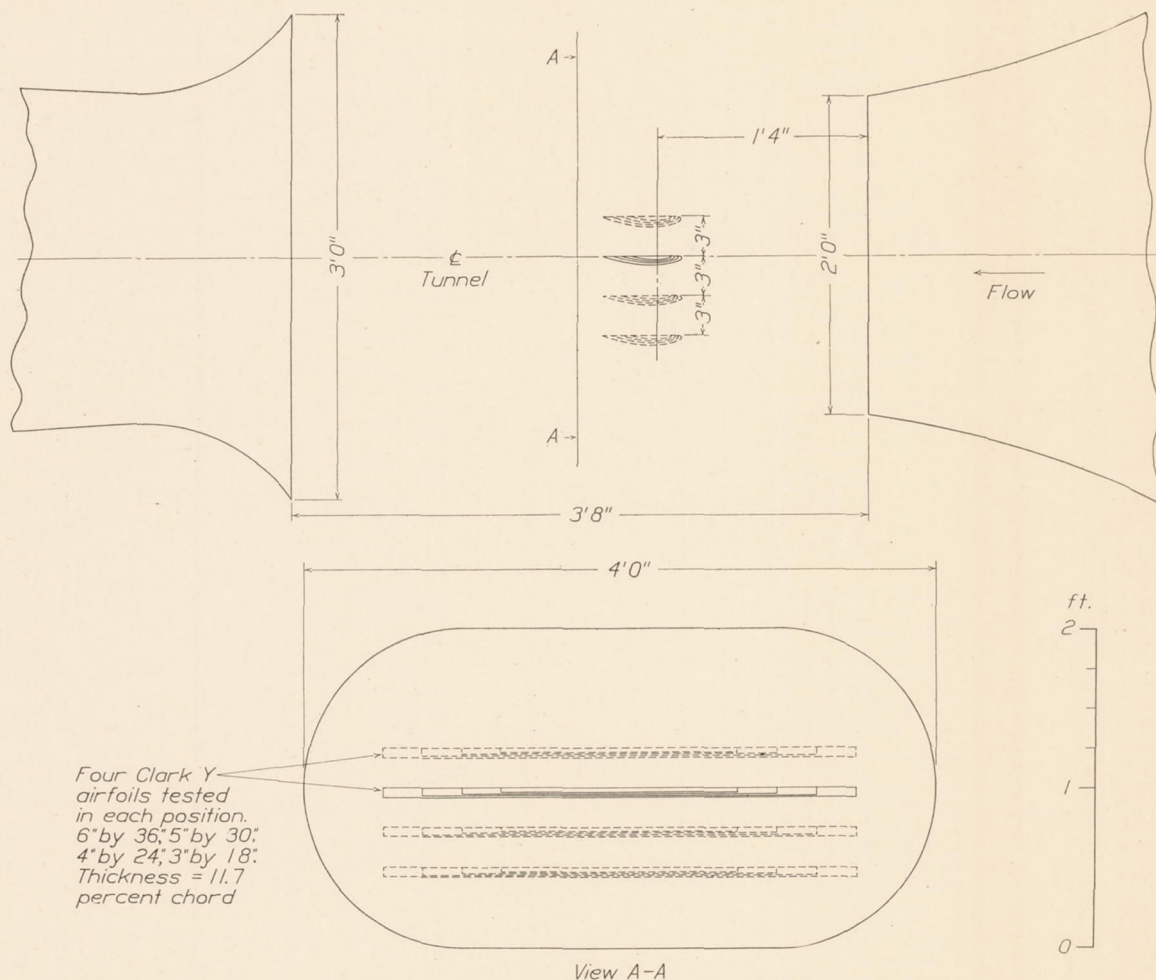

FIGURE 7.—Off-center locations of airfoils in model tunnel.

the airfoils were carefully inspected and measured and no serious irregularities were disclosed.

Tests and results.—The boundary correction factor δ is conventionally defined by the relations,

$$\Delta\alpha = \delta \times \frac{S}{C} \times C_L \qquad (1)$$

and

$$\Delta C_D = \delta \times \frac{S}{C} \times C_L^2 \qquad (2)$$

where $\Delta\alpha$ is the *upward* deflection of the air stream at the airfoil and ΔC_D is the corresponding *decrease* in the drag caused by the presence of the boundaries.

of derivation of the boundary factors, the corresponding plots for the full-scale tunnel will temporarily be made use of here. Figure 27 shows lift and drag against the geometric angle of attack measured from zero lift for the series of four Clark Y airfoils in the full-scale tunnel. The results are extrapolated to a zero value of $\frac{S}{C}$ as illustrated in figure 28. The zero value of $\frac{S}{C}$ corresponds to the free-air condition or the case of zero boundary correction.

It is then possible to plot directly the stream deflection $\Delta\alpha$ and drag decrease ΔC_D against C_L and C_L^2, respectively (fig. 29). Equations (1) and (2) furnish by substitution the experimentally derived values of δ.

It is mentioned at this point that the possible effect of scale was eliminated by using tests of the same Reynolds Number throughout the preceding analysis. The velocities used were 80, 60, 48, and 40 miles per hour for the 3-, 4-, 5-, and 6-inch chord airfoils, respectively. Upright and inverted tests were made for each airfoil to determine the effective tunnel axis.
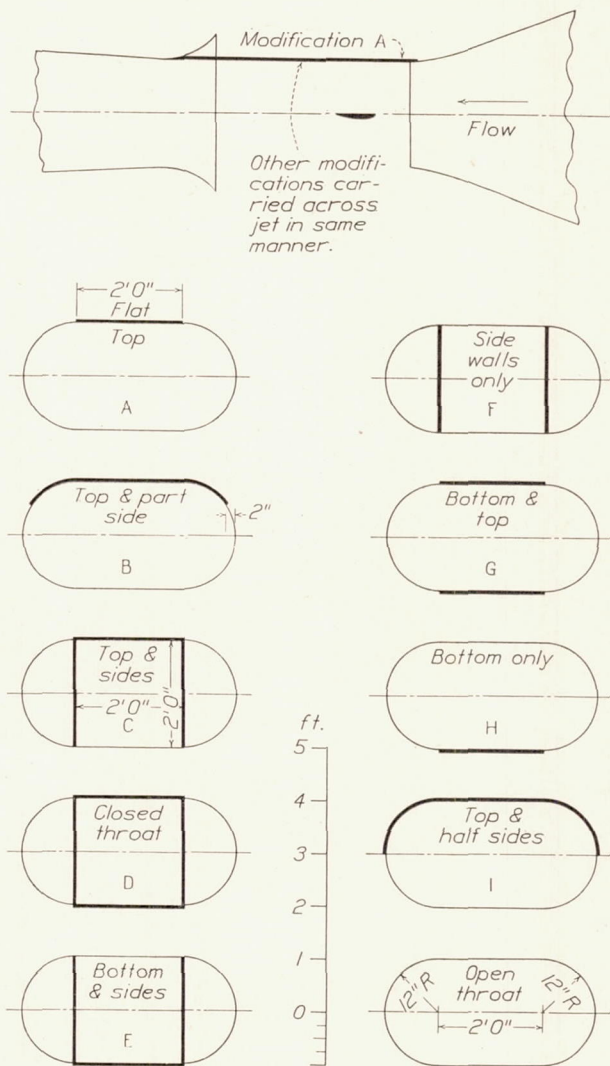

FIGURE 8.—Modifications of model tunnel test chamber.

A total of 29 tests was made in the model tunnel to obtain the desired data. These consisted of the following:

(a) Sixteen tests on the four airfoils, each being tested in four positions in the original tunnel. (Fig. 7 shows positions.)

(b) Thirteen tests to verify the effects of various boundary restraints as predicted in reference 5. These tests were performed in nine modified tunnel types, as lettered from A to I in figure 8. It was necessary in several of the types to restrict the tests to the 3-inch airfoil, inasmuch as the limited width of the tunnel in these cases prohibited the use of an airfoil span in excess of 18 inches.

The results of the tests under (a) are given in figure 9, in which δ_α is the correction factor obtained from equation (1) and δ_D is the correction factor as obtained from equation (2). The curves 1 to 4 refer to the center position in the tunnel. The correction factors δ_α and δ_D are not identical in value. According to theory, no such duplexity is conceded, the values δ in equations (1) and (2) being identical. The remaining tests, 5 to 16, give results for various off-center positions.

The main conclusion to be extracted from this rather chaotic evidence is the fact that the drag correction factors compare, at least approximately, with the theoretical value for the open elliptical tunnel (fig. 1), while the angle correction factors attain entirely too large values. The explanation and detection of the causes of this contradictory result presented themselves as the main objects of the subsequent research.

The results of the tests under (b) are given in figure 10. The tests 1 to 4 have again been included. The airfoils were tested *inverted* in the model tunnel, and this fact should be kept in mind in connection with the tunnel modifications. Test 17 refers to a tunnel with a top boundary only (or bottom with reference to the airfoil), designated modification A on figure 8. Test 18 is taken with the top extended somewhat farther (modification B). It appears from figure 2 that the expected boundary correction in these cases, more particularly the latter, should approximate zero. The experimental results show fair agreement; modification B shows a zero δ_D within experimental error and only a small discrepancy in δ_α at the higher lift coefficients.

Test 20 refers to modification D, which is a closed square tunnel. Figure 1 shows a theoretical value of 1.70 for a square closed tunnel $\lambda = 1$ with a span ratio $\sigma = 0.75$. The experimental result is in perfect agreement for the angle correction factor, δ_α, the value being exactly 1.70; although the drag correction factor, δ_D, is not constant, its average value is close to 1.70.

Test 23 on modification G with top and bottom boundaries shows a theoretical value from figure 2 of approximately zero. The experimental check is not as good, the angle and drag correction factors being of opposite sign and numerically too large.

Tests 24 and 25, representing modifications H and A, must theoretically lie somewhere between the value for a free jet and the value for case V in figure 2. It can be seen that test 24, with a small airfoil, approaches the case of a single horizontal boundary (V), inasmuch as the corrections are both close to zero, while test 25 with a larger airfoil shows values which approach more closely the values for a free jet.

The remaining tunnel modifications show, in general, the expected trends, but since some of these were not treated theoretically and are only of an academic

interest, we shall present the results of these cases with no further comment.

A noteworthy feature of these experiments on modified tunnels is that the deviation from the predicted

A further peculiar result is shown in figure 11, which shows that the maximum lift coefficients for the airfoils tested in the open tunnel decrease with an increase in size. This result was rather unexpected since the
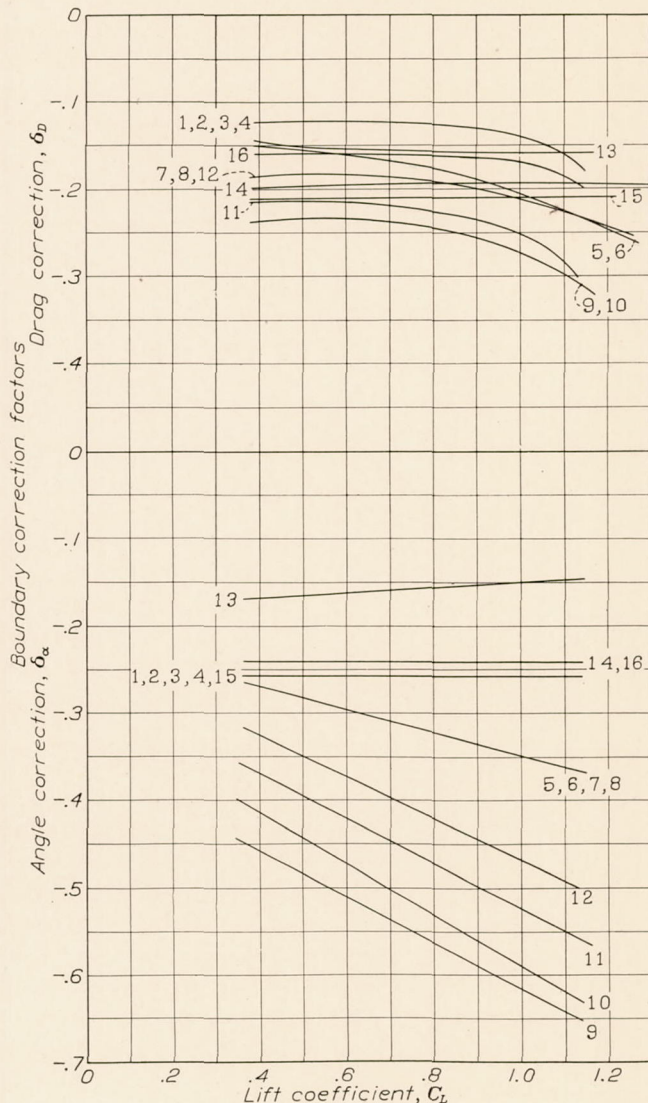

TABLE I

Test no	1	2	3	4	5	6	7	8	9	10	11	12	13	14	15	16
Airfoil	3″	4″	5″	6″	3″	4″	5″	6″	3″	4″	5″	6″	3″	4″	5″	6″
Position	c.l.[1]	c.l.	c.l.	c.l.	3″ below c.l.				6″ below c.l.				3″ above c.l.			
S/C	0. 053	0. 094	0. 146	0. 210	0. 053	0. 094	0. 146	0. 210	0. 053	0. 094	0. 146	0. 210	0. 053	0. 094	0. 146	0. 210

[1] Center line.

Note.—Airfoils tested in inverted position for above test.

FIGURE 9.—Angle and drag correction factors for the original model tunnel. (See table I.)

values becomes larger for partially and fully open tunnels, while quite close agreement is obtained for the closed type. The drag coefficient shows again the best agreement with the predicted values. The open tunnel (tests 1 to 4) shows the largest corrections.

tests were conducted at a given Reynolds Number and in the same tunnel. Obviously, some influence is present which has not formerly been considered.

It is evident from the preceding paragraphs that no really satisfactory agreement was obtained between
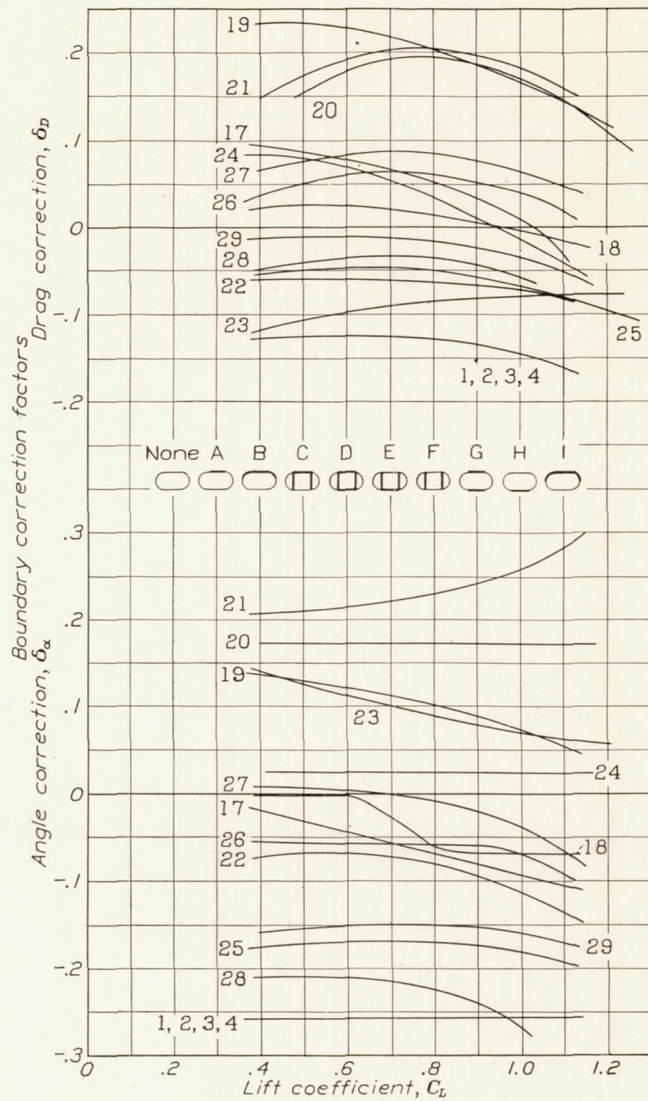
TABLE II

Test no	1	2	3	4	17	18	19	20	21
Airfoil	3″	4″	5″	6″	3″	3″	3″	3″	3″
Position	c.l.[1]	c.l.	c.l.	c.l.	c.l.	c.l.	c.l.	c.l.	c.l.
Type of tunnel wall [2]	None	None	None	None	Top	Top and part side.	Top and sides	Closed tunnel	Bottom and sides.
Modification					A	B	C	D	E

Test no	22	23	24	25	26	27	28	29
Airfoil	3″	3″	3″	6″	6″	6″	6″	4″
Position	c.l.	c.l.	c.l.	c.l.	c.l.	c.l.	c.l.	c.l.
Type of tunnel wall [2]	Sides	Top and bottom.	Bottom	Top	Top and part sides.	Top and half sides.	Top and half sides.	Top.
Modification	F	G	H	A	B	I	I	A

[1] Center line.   [2] See fig. 8 for descriptive drawings.

NOTE.—Airfoils in inverted position for above tests.

FIGURE 10.—Angle and drag correction factors for various modifications of the model tunnel. (See table II.)

the experimental and the theoretically predicted boundary correction factors of the model tunnel. It was at the time believed that the low Reynolds Number might have had an objectionable effect on the results, and also that the test accuracy in this small tunnel might not have been sufficient. The unexpected effect on the maximum lift and the consistently larger errors in the boundary factors for the open tunnels rather tended to indicate that a more fundamental cause was to be suspected.

FULL-SCALE TUNNEL INVESTIGATION

Tunnel and equipment.—The full-scale tunnel and its equipment have been fully described in reference 6. The cross section of the jet, which is similar to that of the model tunnel, is of a width/height ratio of 2, with parallel top and bottom and semicircular ends (figs. 12 and 13). The jet is 60 feet wide and 30 feet high, and has a free length of 56 feet between entrance and exit c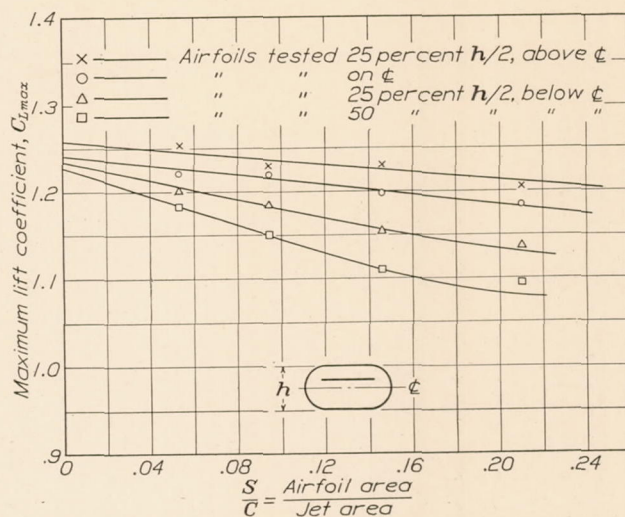ones. Two electric motors enclosed in stream-line nacelles circulate the air through the tunnel. A 6-component electrically recording balance measures

FIGURE 11.—Variation in maximum lift coefficient in model tunnel for various positions of airfoils.
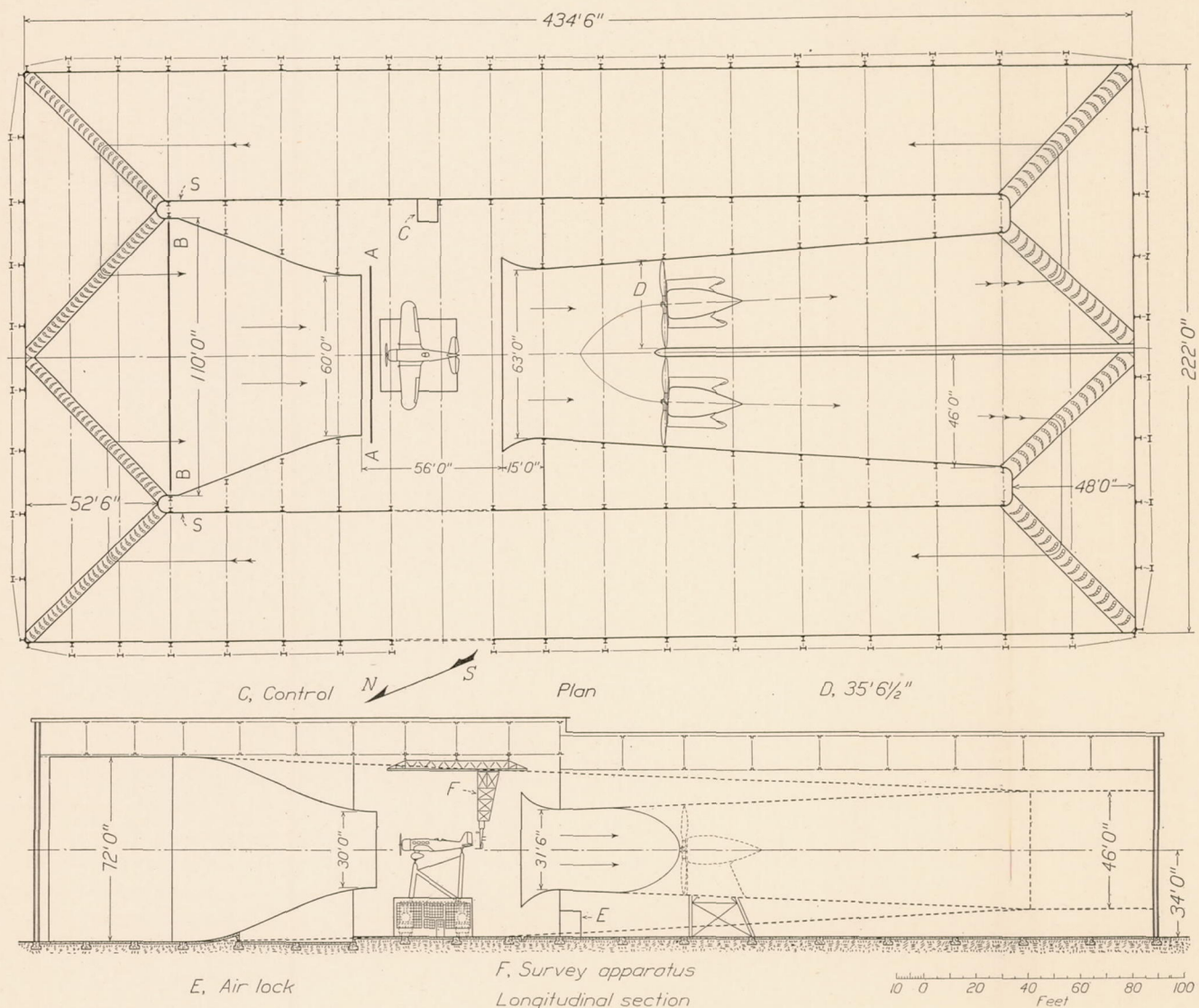
FIGURE 12.—Plan and elevation of full-scale tunnel.

and records the forces and moments. The airfoil is supported in the air stream on the balance frame by streamlined struts (fig. 13). Careful shielding of the
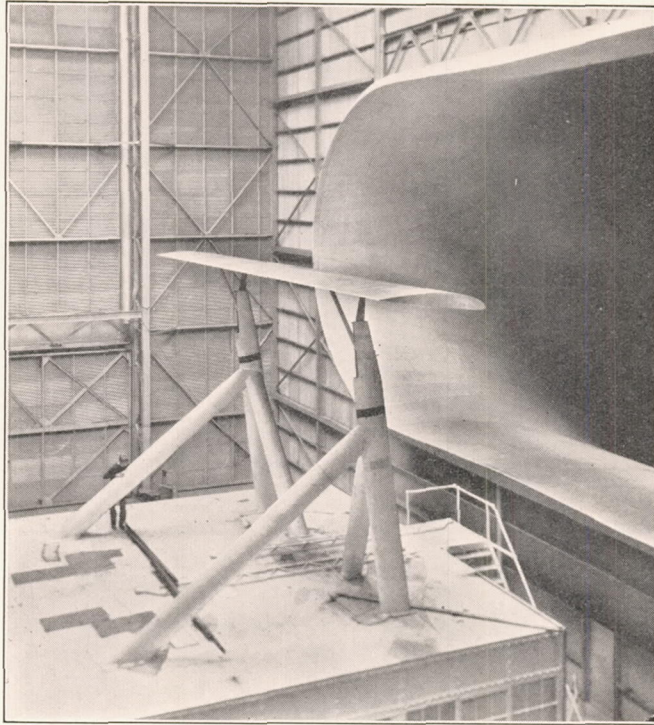

FIGURE 13.—Experimental set-up of Clark Y airfoil in full-scale tunnel.

major portion of these supporting struts and streamlining of all exposed surfaces reduce the tare drag to a low value (about one third of the minimum airfoil drag for the smallest airfoil and one fiftieth of the
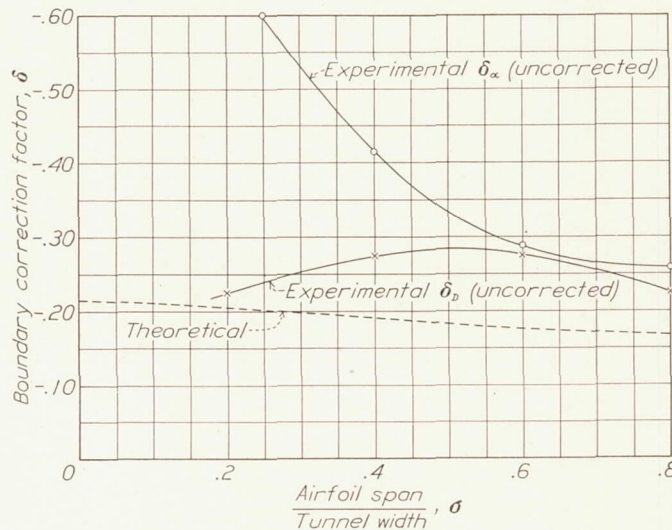

FIGURE 14.—Preliminary results on the boundary corrections for the full-scale tunnel

minimum drag of the largest airfoil). The arrangement and method of measuring dynamic pressures are similar to those of the model. The location of the static pressure orifices is shown at S on figure 12.

Four Clark Y airfoils, which were especially built for the purpose, were used as standards throughout the

entire series of tests. These served, in addition, the important purpose of furnishing the full-scale characteristics of the Clark Y airfoil. The airfoils are of 12-, 24-, 36-, and 48-foot span, all with an aspect ratio of 6, constructed with steel spars and aluminum sheet covering. These airfoils were also subjected to a careful inspection and checking, and were found to comply with the stringent requirements of this type of experiment.

Preliminary results.—The initial results from the full-scale tunnel boundary correction tests are shown in figure 14. The extrapolation process and detailed procedure are the same as those outlined for the model-tunnel tests. It is observed that the agreement with the predicted theoretical value is no better than in the case of the model tunnel. It became evident at this point that the difficulty could not all be due to scale effect or test inaccuracy, as the experimental test accuracy of the full-scale tunnel was considerably
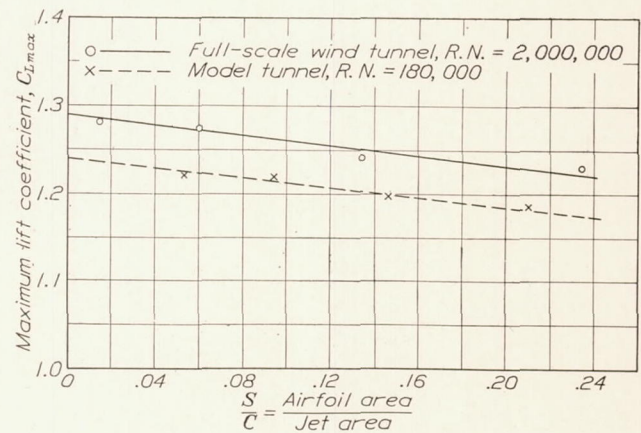

FIGURE 15.—Variation of maximum lift with airfoil size in full-scale tunnel.

greater than that of the model tunnel, and the Reynolds Number about 15 times larger.

Considerable time and effort were spent in arriving at the correct explanation of the large discrepancy with the theoretically predicted results. The possible effect of the load distribution over the airfoil was considered, but discarded as being of negligible importance. A number of possible effects, such as curvature of the stream, length of the free jet, the effect of the exit cone restraint, and spillage, were theoretically considered; but none of them was found to be of appreciable concern.

A further definite agreement with the results from the model tunnel in regard to maximum lift coefficient is shown in figure 15, in which the upper curve shows the results in the full-scale tunnel. The values of the maximum lift coefficient in the large tunnel are greater, as expected, but the considerable drop in the maximum lift with increase in airfoil size persists. From the earlier results in the model tunnel it was already established (fig. 11) that certain off-center stations of the airfoil resulted in still smaller lift coefficients. It

was suspected that this effect was intimately related to the discrepancies in the boundary correction factors.

Dynamic pressure or q correction.—It was recognized at this time that an error in the measurement of the velocity head might account not only for the drop in maximum lift but also for the discrepancies in the boundary correction factors. The calibration of the tunnel had been, as is conventional, performed with the jet *empty*, with the tacit assumption that this cali-
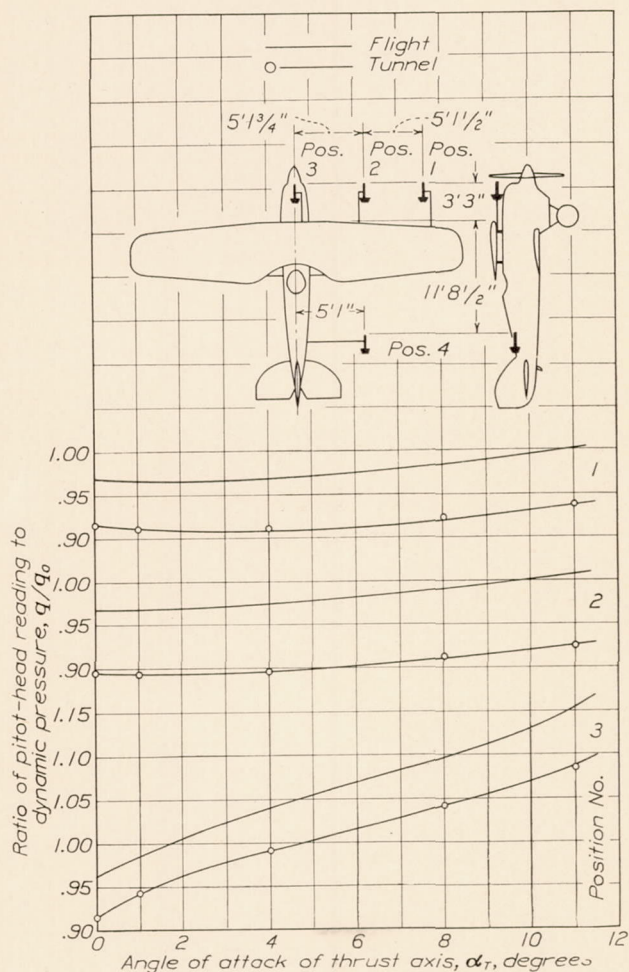

FIGURE 16.—Dynamic pressure at three locations on the PW–9 airplane in flight and in the full-scale tunnel. q_o, dynamic pressure in flight or in the tunnel; q, local dynamic pressure.

bration sufficed for the tests with a body in the air stream. Although nothing but the ordinary displacement blocking was anticipated it was decided to subject the problem to an exhaustive investigation.

Figure 12 shows the location of a full-size airplane in the large tunnel. A pitot tube was attached to the wing of an airplane in the full-scale tunnel, well in front of the wing and clear of the body. The indicated dynamic pressure on this pitot head showed the astonishing result of reading about 7 percent below the estimated theoretical value, apparently indicating a considerable decrease in velocity in the region around the airplane.

In order to substantiate this finding and to avoid the necessity of theoretical estimates of the velocity field, it was decided to obtain a direct comparison with flight. A PW–9 airplane was equipped with four pitot heads, as shown in figure 16, and observations of the dynamic and static pressures at these locations were taken in flight over a large angle-of-attack range. The airplane was then installed in the tunnel and identical observations taken. The results, shown in figures 16 and 17, confirm beyond question the existence of a considerable distortion of the velocity field in the tunnel. Figure 16 shows the dynamic pressure for three front locations. Figure 17 shows the static pressure for the same three locations, using the static
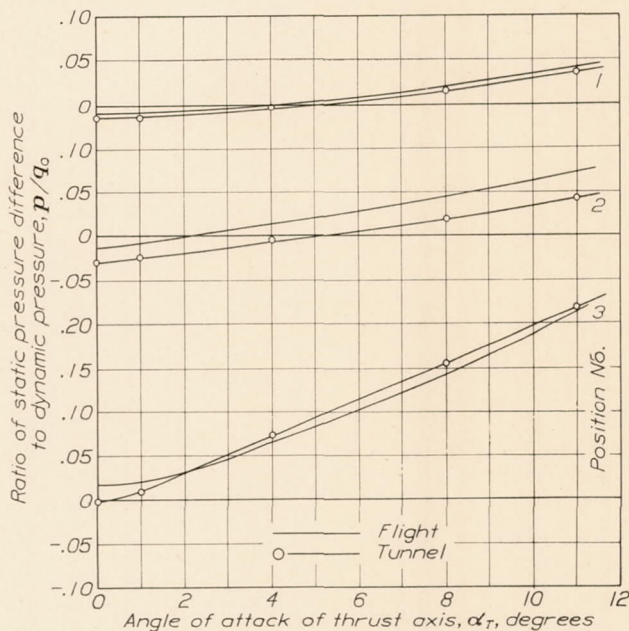

FIGURE 17.—Static pressure at three locations on the PW–9 airplane in flight and in the full-scale tunnel. Static pressure at rear pitot head no. 4 used as reference. q_o, dynamic pressure in flight or in the tunnel; p, local static pressure minus the static pressure at head no. 4.

head at the fourth (rear) pitot tube as a reference pressure. The differences between the static pressures taken in flight and in the tunnel are shown plotted along the span in figure 18. Observe that the average dynamic pressure in the region around the airplane is about 6 percent lower than that of flight, when the indicated tunnel velocity is equal to the flight speed. Observe also that there is a static gradient in the tunnel acting in a direction so as to increase the drag force. This latter effect is of the order of 5 percent of the minimum drag.

The velocity field in the tunnel was subsequently studied in greater detail. Figures 19, 20, and 21 show, respectively, the dynamic, static, and total pressures taken with the full-scale tunnel survey equipment (reference 6) at position A (fig. 12) approximately 13 feet ahead of the PW–9 airplane, which has a 32-foot span. Notice the large velocity drop in the

central part of the jet in figure 19 and the static pressure increase in figure 20. The reference pressure for static measurement is the pressure in the tunnel test chamber. The total head in figure 21 shows a definite decrease toward the center of the air stream, indicating
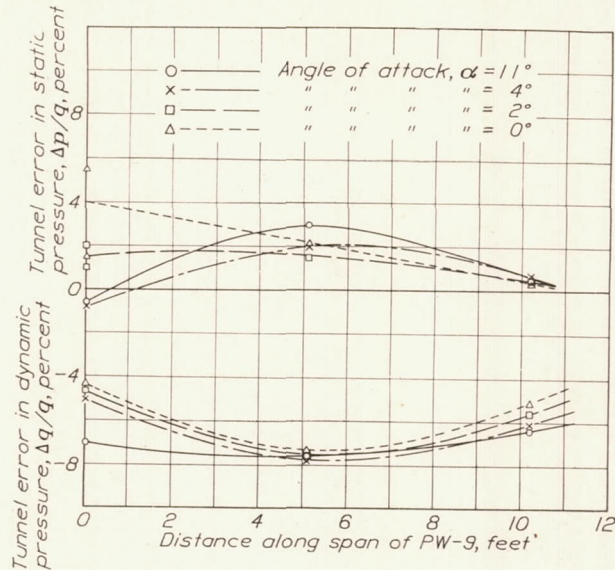

FIGURE 18.—Blocking errors along the span of the PW–9 airplane at different angles of attack in the jet of the full-scale tunnel.

that the energy in the region around the airplane is below that of the exterior jet from which the indicated tunnel velocity is obtained.

This decrease in velocity head obtained with the survey apparatus is within about 1 percent of that indicated by the pitot heads on the airplane, showing
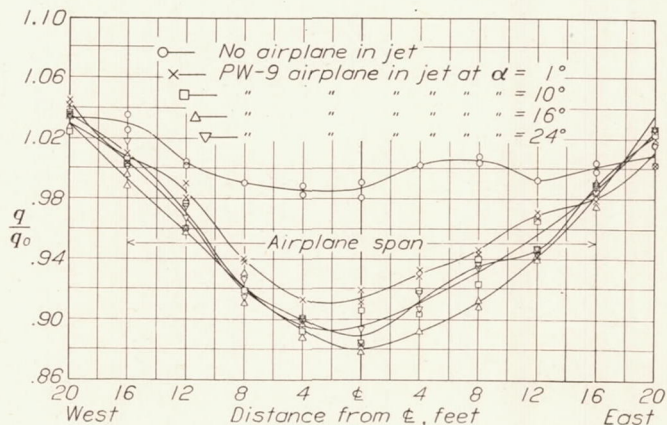

FIGURE 19.—Dynamic-pressure surveys at wing height and two chords in front of the PW–9 airplane in the full-scale tunnel. q_o, average dynamic pressure along the span with jet empty; q, dynamic pressure with the airplane in the tunnel.

that the effect is not localized to the immediate vicinity of the airplane. It was therefore suspected that the effect might extend much farther in the forward direction. This suspicion was substantiated. Figure 22 shows the velocity distribution at the large end of the entrance cone (at section B–B in fig. 12) resulting from the PW–9 at several angles of attack, as compared with that of the empty tunnel. It becomes

obvious that the characteristics of an airplane determined with disregard of this considerable field distortion are in error. Both the slope of the lift curve and the maximum lift coefficient become too low, simply because they are computed on the basis of a velocity
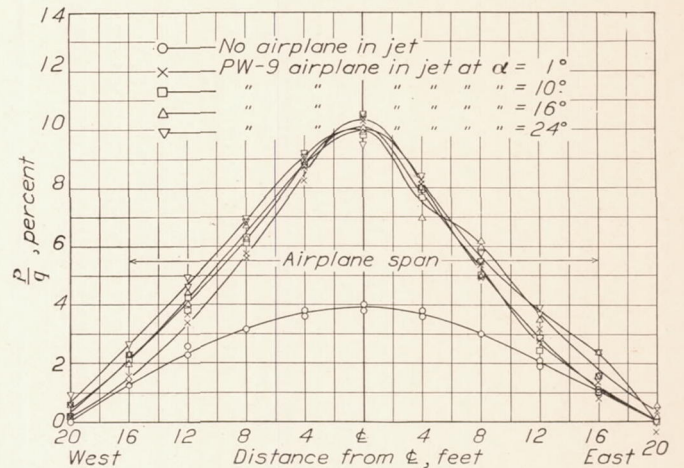

FIGURE 20.—Static-pressure surveys at wing height and two chords in front of the PW–9 airplane in the full-scale tunnel. p, static pressure in jet with reference to the test chamber; q, dynamic pressure in the jet.

higher than that existing. The drag coefficients are affected in essentially the same manner; however, the effect of the static pressure gradient must also be included.

The definition of the true velocity in a distorted field of this nature becomes quite difficult. A permissible approximation may be to use the average velocity
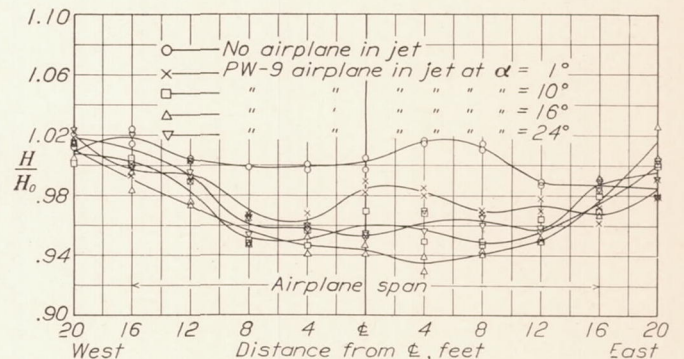

FIGURE 21.—Total-pressure surveys at wing height and two chords in front of the PW–9 airplane in the full-scale tunnel. H_o, average total pressure along the span with jet empty; H, total pressure with the airplane in the tunnel.

along the span taken at some distance in front of the airplane. This average velocity is, as pointed out, considerably below the indicated tunnel velocity, necessitating a considerable correction to the latter. It will in the following be referred to as a "q" correction.

Support interference.—The necessity in a problem of this nature for reducing all errors to an absolute minimum forced a further inquiry. When comparing tests with airfoils in upright and inverted positions, that is, with the supports attached to the lower and upper surfaces respectively, it was observed that a

good agreement in the characteristics of the smaller airfoils did not result. The drag of the supports was measured separately with the airfoil in position, but
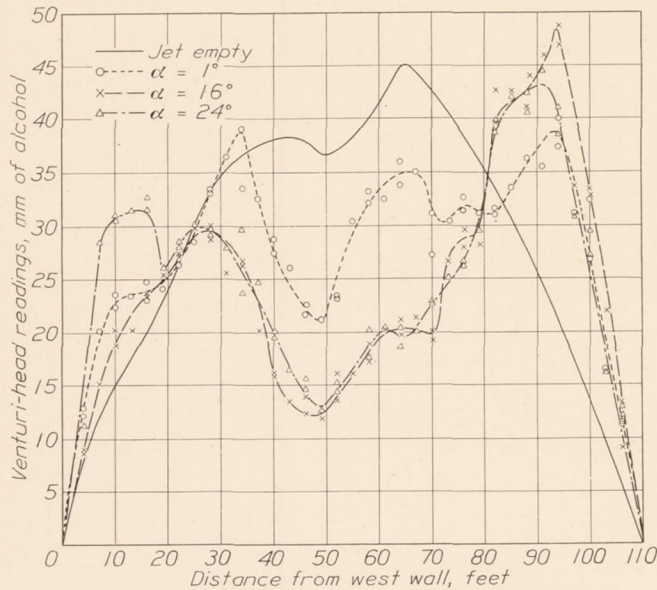

FIGURE 22.—Velocity distribution showing the blocking effect extending into the mouth of the entrance cone.

supported by wires. This drag of the exposed struts, which included the interference of the wing upon them, was subtracted from the drag of the total set-up.
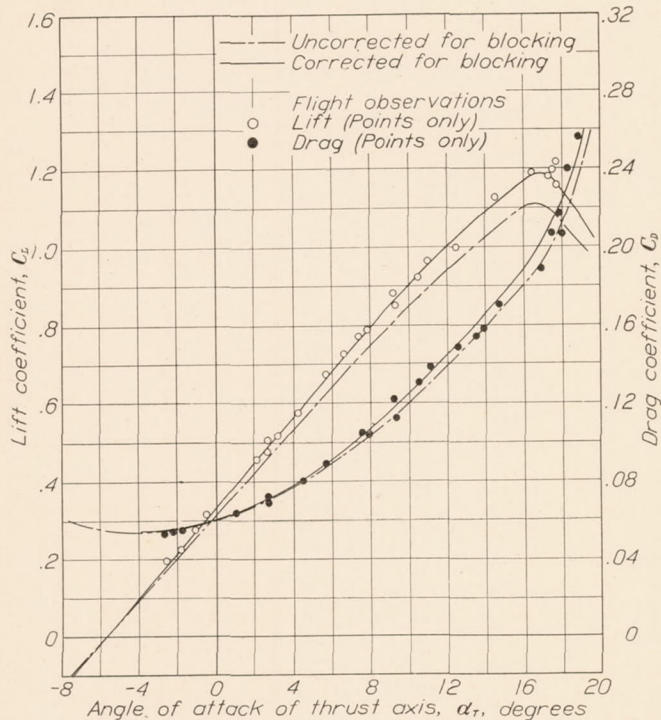

FIGURE 23.—Characteristics of the PW–9 airplane obtained in the full-scale tunnel, corrected for blocking and boundary interference, and compared with flight results.

It was acknowledged that the difference in the results was due to the interference of the supports upon the airfoil, although at first it was difficult to imagine that

the effect of these unusually small and carefully stream-lined supports (fig. 13) could be of any consequence. It was found that in the *upright* position the drag at zero lift was increased by a large unfavorable interference effect due to the struts. The *inverted* position showed an apparent, although small, favorable interference. This latter result was found to be produced by a virtual straightening of the effective mean camber line of the airfoil. It was necessary to resort to the refinement of adding dummy supports to the opposite side of the airfoil. The results from the upright and inverted tests were thus brought into satisfactory agreement. Details of these tests will be published in a future paper.

Boundary-correction factor.—With the establishment of the existence of the q correction for the full-scale tunnel, the predicted boundary correction factors were successfully applied to a number of airplanes for which flight data were available. Figure 23, showing
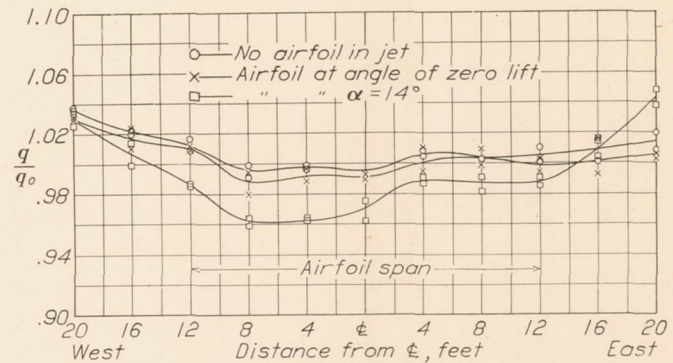

FIGURE 24.—Dynamic-pressure surveys level with and approximately three chords in front of the by 4- by 24-foot airfoil. q_o, average dynamic pressure along the span with jet empty; q, dynamic pressure with the airfoil in the tunnel.

comparative results of the characteristics of the PW–9 airplane from tunnel and flight tests, is presented as an example. The lift and drag values obtained in flight are shown with points only. The broken curves show the wind-tunnel tests corrected for jet boundaries, while the continuous curves take the q correction also into account. The agreement is striking.

Similar results giving the comparison between flight and tunnel tests on the Fairchild F–22 airplane are presented in reference 6. Good agreement has also been obtained on the YO–31A and several other airplanes employing an estimated value of the q correction. It is worthy of notice that the maximum lifts in all cases were brought into close agreement with flight results by means of the q correction.

It was of interest to determine the q correction to be applied to the standard airfoil series. It was necessary, of course, to make a theoretical estimate of the undisturbed field around the airfoil, as no flight observations could possibly be obtained. The 24- and the 48-foot airfoils were checked.

Figures 24, 25, and 26 show the dynamic pressure, static head, and total head as measured approximately

12 feet ahead of the 4- by 24-foot airfoil. The average drop in the dynamic pressure across the span varies from a negligible quantity at low angles to about
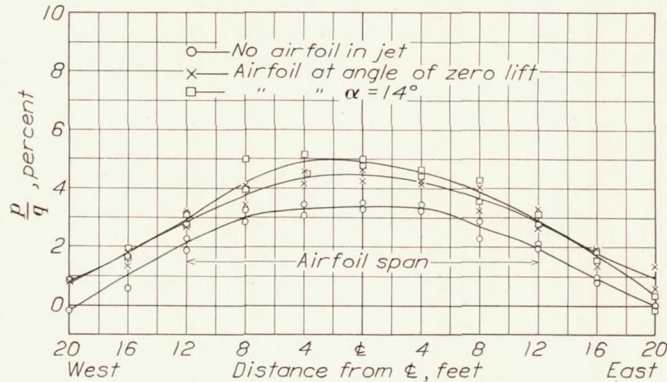

FIGURE 25.—Static-pressure surveys level with and approximately three chords in front of the 4- by 24-foot airfoil. p, static pressure in jet with reference to the test chamber; q, dynamic pressure in the jet.

3 percent at high angles. The experimental angle and drag correction factors were found to be equal and to fall close to the predicted curve. (See circles in fig. 30.)
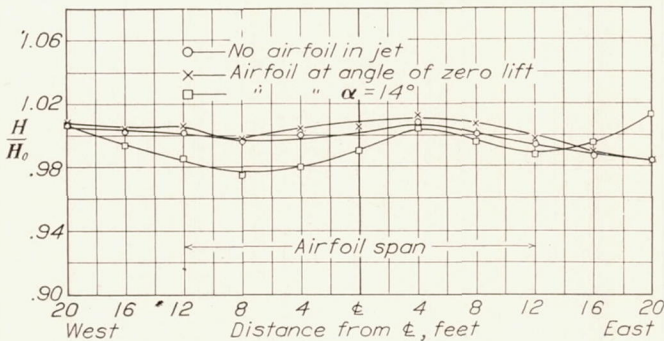

FIGURE 26.—Total-pressure surveys level with and approximately three chords in front of the 4- by 24-foot airfoil. H_o, average total pressure along the span with jet empty; H, total pressure with the airfoil in the tunnel.

An explanation of the curious drop in maximum lift with the size of the airfoil (fig. 15) is available. By introducing the correct value of the velocity for the 4 by 24 and 8 by 48 airfoils from the surveys, no drop in maximum lift is obtained. On assuming a direct relationship between the velocity decrease and the decrease in maximum lift for the remaining airfoils, the boundary correction factors fall into agreement with the theory (fig. 30). Figures 27, 28, and 29 show the intermediate steps in the derivation.

CONCLUDING REMARKS

It has thus been shown that the predicted boundary factors are confirmed, provided that proper account is taken of strut interference and velocity errors. The adequacy of the theory has thus been verified.

Regarding the real nature of the q correction, it is recognized that it differs from the usual displacement
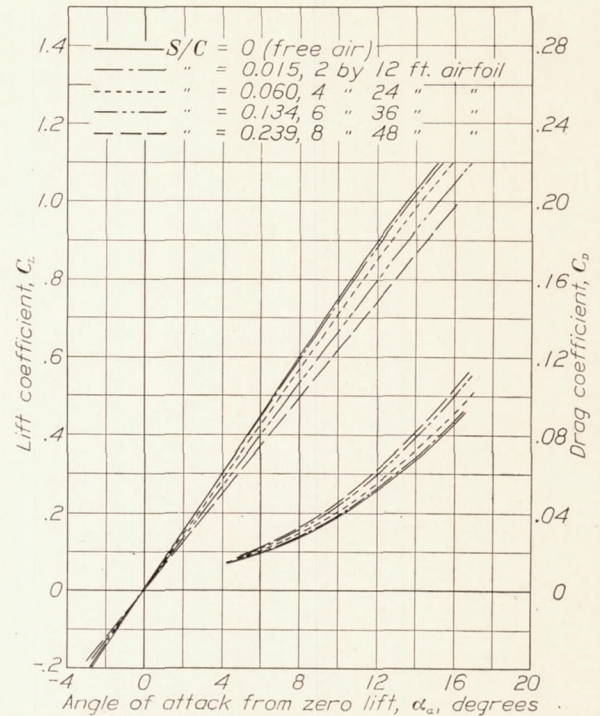

FIGURE 27.—Lift and drag coefficients of four Clark Y airfoils obtained in the full-scale tunnel, corrected for tunnel blocking.
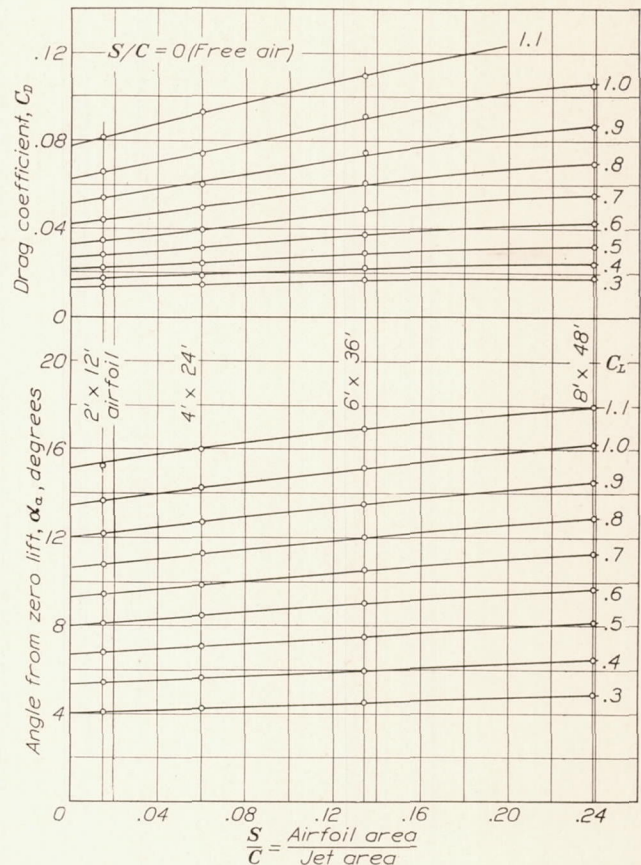

FIGURE 28.—Extrapolation of corrected airfoil characteristics to free-air condition.

blocking. The large distortion at the mouth of the entrance cone, almost 100 feet ahead of the test section, excludes the possibility that this is the normal type of blocking, since the effect of the normal displacement blocking is confined to the immediate vicinity of the object. The decrease in dynamic pressure observed in front of the test body is associated with a corresponding, but much smaller, increase in static pressure, resulting in a deficiency of total head.
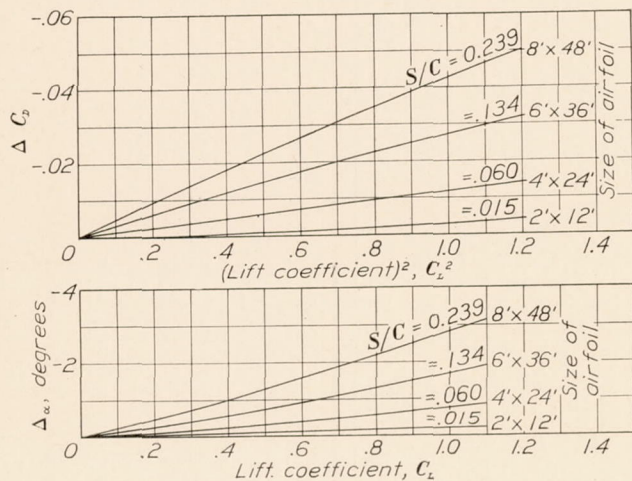

FIGURE 29.—Down-flow angle and drag increment against lift coefficient.

The loss in total head seems to account for the greater part of the q correction. Quite evidently the pattern, or wake of the body, is carried around the tunnel. It is not inconceivable that this considerable wake might be responsible for a further distortion of the flow in the entrance cone. It is realized that the flow in a short entrance cone is of a rather unstable nature, and that the introduction of a slower moving core might tend to upset the normal flow.

While it is believed that a wake could build up and persist in a tunnel with small inherent turbulence, it is obvious that such a pattern would be rapidly dissipated in a more turbulent tunnel. It is probable that a velocity distortion of this kind might be a contributing factor to the differences in maximum lift coefficients observed in various tunnels.

No attempt has been made to extend this study to provide a basis for the prediction of the q correction or to the avoidance of this phenomenon. It will be a problem for future experience and research to determine
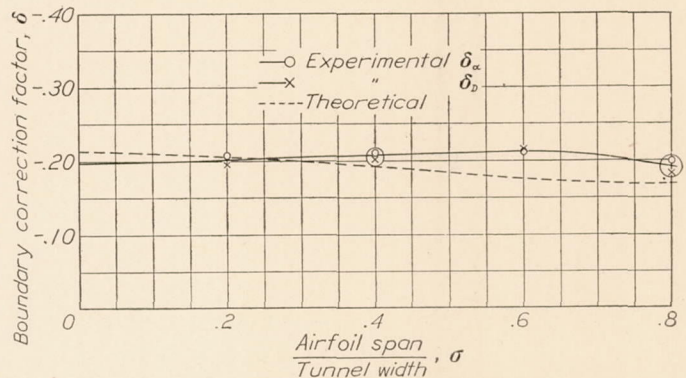

FIGURE 30.—Experimental and theoretical boundary-correction factors for the full-scale tunnel. Points in large circles obtained by direct measurement of blocking. Remaining points obtained on basis of blocking as indicated by drop in maximum lift.

in what manner the velocity distortion depends on the characteristics of the body and the tunnel.

LANGLEY MEMORIAL AERONAUTICAL LABORATORY,
NATIONAL ADVISORY COMMITTEE FOR AERONAUTICS,
LANGLEY FIELD, VA., *May 18, 1933.*

REFERENCES

1. Tani, Itiro, and Sanuki, Matao: The Wall Interference of a Wind Tunnel of Elliptic Cross-Section. Proceedings of the Physics-Math. Soc. of Japan, 3d Series, vol. 14, no. 10, 1932.
2. Glauert, H.: Interference on Characteristics of Aerofoil in Wind Tunnel of Rectangular Section. R. & M. No. 1459, British A.R.C., 1932.
3. Theodorsen, Theodore: Interference on an Airfoil of Finite Span in an Open Rectangular Wind Tunnel. T.R. No. 461, N.A.C.A., 1933.
4. Knight, Montgomery, and Harris, Thomas A.: Experimental Determination of Jet Boundary Corrections for Airfoil Tests in Four Open Wind Tunnel Jets of Different Shapes. T.R. No. 361, N.A.C.A., 1930.
5. Theodorsen, Theodore: The Theory of Wind-Tunnel Wall Interference. T.R. No. 410, N.A.C.A., 1931.
6. DeFrance, Smith J.: The N.A.C.A. Full-Scale Wind Tunnel. T.R. No. 459, N.A.C.A., 1933.
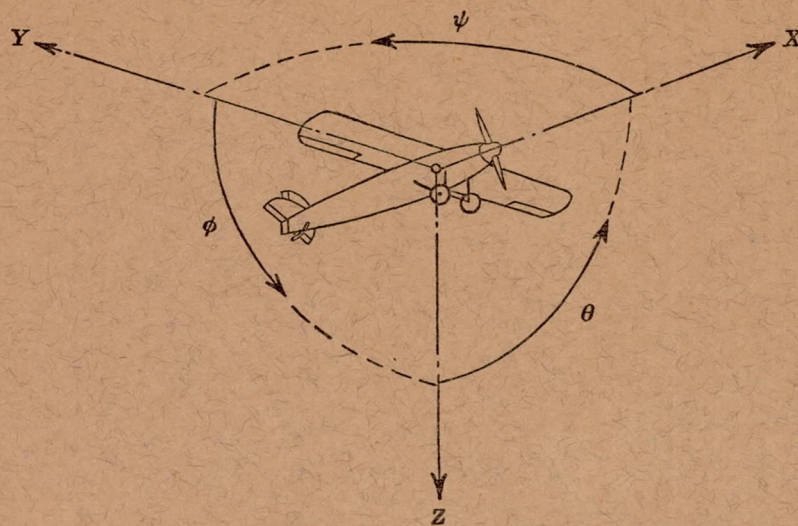
Positive directions of axes and angles (forces and moments) are shown by arrows

Axis		Force (parallel to axis) symbol	Moment about axis			Angle		Velocities	
Designation	Symbol		Designation	Symbol	Positive direction	Designation	Symbol	Linear (component along axis)	Angular
Longitudinal	X	X	Rolling	L	$Y \longrightarrow Z$	Roll	ϕ	u	p
Lateral	Y	Y	Pitching	M	$Z \longrightarrow X$	Pitch	θ	v	q
Normal	Z	Z	Yawing	N	$X \longrightarrow Y$	Yaw	ψ	w	r

Absolute coefficients of moment

$$C_l = \frac{L}{qbS} \qquad C_m = \frac{M}{qcS} \qquad C_n = \frac{N}{qbS}$$

(rolling)   (pitching)   (yawing)

Angle of set of control surface (relative to neutral position), δ. (Indicate surface by proper subscript.)

4. PROPELLER SYMBOLS

D, Diameter
p, Geometric pitch
p/D, Pitch ratio
V', Inflow velocity
V_s, Slipstream velocity

T, Thrust, absolute coefficient $C_T = \dfrac{T}{\rho n^2 D^4}$

Q, Torque, absolute coefficient $C_Q = \dfrac{Q}{\rho n^2 D^5}$

P, Power, absolute coefficient $C_P = \dfrac{P}{\rho n^3 D^5}$

C_s, Speed-power coefficient $= \sqrt[5]{\dfrac{\rho V^5}{Pn^2}}$

η, Efficiency
n, Revolutions per second, r.p.s.

Φ, Effective helix angle $= \tan^{-1}\left(\dfrac{V}{2\pi rn}\right)$

5. NUMERICAL RELATIONS

1 hp. = 76.04 kg-m/s = 550 ft-lb./sec.
1 metric horsepower = 1.0132 hp.
1 m.p.h. = 0.4470 m.p.s.
1 m.p.s. = 2.2369 m.p.h.

1 lb. = 0.4536 kg.
1 kg = 2.2046 lb.
1 mi. = 1,609.35 m = 5,280 ft.
1 m = 3.2808 ft.